

Heterobimetallic Bi(III)–Ti(IV) Coordination Complexes: Synthesis and Solid-State Structures of $\text{BiTi}_4(\text{sal})_6(\mu\text{-O}^i\text{Pr})_3(\text{O}^i\text{Pr})_4$, and the Cyclic Isomers $\text{Bi}_4\text{Ti}_4(\text{sal})_{10}(\mu\text{-O}^i\text{Pr})_4(\text{O}^i\text{Pr})_4$ and $\text{Bi}_8\text{Ti}_8(\text{sal})_{20}(\mu\text{-O}^i\text{Pr})_8(\text{O}^i\text{Pr})_8$

John H. Thurston, Arvind Kumar, Cristina Hofmann, and Kenton H. Whitmire*

Department of Chemistry, Rice University, Houston, Texas 77005

Received July 15, 2004

The reaction of a 1:2 mixture of bismuth(III) salicylate with titanium(IV) isopropoxide in refluxing toluene has been investigated and found to proceed with ligand exchange to produce the new heterobimetallic complexes $\text{BiTi}_4(\text{sal})_6(\mu\text{-O}^i\text{Pr})_3(\text{O}^i\text{Pr})_4$ (**1**), $\text{Bi}_4\text{Ti}_4(\text{sal})_{10}(\mu\text{-O}^i\text{Pr})_4(\text{O}^i\text{Pr})_4$ (**2**), and $\text{Bi}_8\text{Ti}_8(\text{sal})_{20}(\mu\text{-O}^i\text{Pr})_8(\text{O}^i\text{Pr})_8$ (**3**). Complex **1** is the major product, while **2** and **3** were identified as minor products from the reaction. Compound **1** is produced pure and in high yield by employing stoichiometric amounts of reagents; its crystal structure consists of a $[\text{Ti}_4(\text{sal})_6(\text{O}^i\text{Pr})_7]^{3-}$ ion capped by a Bi^{3+} ion. Complexes **2** and **3** exhibit cyclic ring structures of bismuth and titanium atoms showing crystallographically imposed inversion symmetry. Both structures occlude large quantities of lattice solvent. The compositional and structural parameters from the single crystal studies indicate that complexes **2** and **3** may represent sequential steps in a ligand exchange process between the two metal species, while the reactivity patterns that were observed provide clues about the solution state structure of bismuth(III) salicylate itself. The 2D COSY ^1H NMR spectrum of **1** indicates retention of the asymmetric structure in solution as evidenced by the presence of 14 diastereotopic isopropoxide methyl resonances.

Introduction

Bimetallic and multimetallic oxide systems are being explored for numerous applications including the development of new nonlinear optics¹ and ferroelectric and piezoelectric materials,² and for the exceptionally high ion mobility some of these systems exhibit in the solid state.³ Furthermore, heterometallic bismuth oxides have been utilized as oxidation catalysts⁴ and high T_c superconductors.^{5,6} Of particular significance are the bismuth titanates $\text{Bi}_4\text{Ti}_3\text{O}_{12}$, $\text{Bi}_2\text{Ti}_4\text{O}_{11}$, and $\text{Bi}_2\text{Ti}_2\text{O}_7$, which are being investigated for their electronic properties including ferroelectric and antiferroelectric characteristics.^{7–16}

It is widely recognized that the conditions under which these materials are synthesized can have a profound effect on the chemical and physical properties of the products. Moreover, there is significant evidence indicating that oxide-based materials produced by wet chemical approaches have superior properties to those generated by traditional solid-state techniques.^{17,18} Specific examples include reports that

* To whom correspondence should be addressed. E-mail: whitmir@rice.edu. Phone: 713-348-5650. Fax: 713-348-5155.

- (1) Parola, S.; Papiernik, R.; Hubert-Pfalzgraf, L. G.; Bois, C. *J. Chem. Soc., Dalton Trans.* **1998**, 737–739.
- (2) Zhou, Q. F.; Chan, H. L. W.; Choy, C. L. *J. Non-Cryst. Solids* **1999**, *254*, 106–111.
- (3) Pell, J. W.; Davis, W. C.; zur Loye, H. C. *Inorg. Chem.* **1996**, *35*, 5754–5755.
- (4) Ono, T. *J. Catal.* **1998**, *175*, 185–93.
- (5) Maeda, H.; Tanaka, Y.; Fukutomi, M.; Asano, T. *Jpn. J. Appl. Phys.* **1988**, *27*, L209.
- (6) Hodge, P.; James, S.; Norman, N.; Orpen, A. *J. Chem. Soc., Dalton Trans.* **1998**, 4049–4054.
- (7) Liu, J.; Duan, C.-G.; Yin, W.-G.; Mei, W. N.; Smith, R. W.; Hardy, J. R. *J. Chem. Phys.* **2003**, *119*, 2812–2819.

- (8) Su, W.-F.; Lu, Y.-T. *Mater. Chem. Phys.* **2003**, *80*, 632–637.
- (9) Jiang, A. Q.; Zhang, L. D. *Phys. Rev. B: Condens. Matter* **1999**, *60*, 9204–9207.
- (10) Chon, U.; Jang, H. M.; Park, I. W. *Solid State Commun.* **2003**, *127*, 469–473.
- (11) Hou, Y.; Wang, M.; Xu, X.-H.; Wang, D.; Wang, H.; Shang, S.-X. *J. Am. Ceram. Soc.* **2002**, *85*, 3087–3089.
- (12) Matsuda, H.; Ito, S.; Iijima, T. *Mater. Res. Soc. Symp. Proc.* **2003**, *748*, 349–359.
- (13) Shibuya, A.; Noda, M.; Okuyama, M. *Mater. Res. Soc. Symp. Proc.* **2003**, *748*, 393–398.
- (14) Takahashi, M.; Noguchi, Y.; Miyayama, M. *Jpn. J. Appl. Phys., Part 1* **2002**, *41*, 7053–7056.
- (15) Van Bael, M. K.; Nelis, D.; Hardy, A.; Mondelaers, D.; Van Werde, K.; D'Haen, J.; Vanhoyland, G.; Van Den Rul, H.; Mullens, J.; Van Poucke, L. C.; Frederix, F.; Wouters, D. *J. Integr. Ferroelectr.* **2002**, *45*, 113–122.
- (16) Yamaguchi, M.; Nagatomo, T.; Masuda, Y. Proceedings of the IEEE International Symposium on Applications of Ferroelectrics, 13th, Nara, Japan, May 28–June 1, 2002; pp 231–234.
- (17) Gopalakrishnan, J. *Chem. Mater.* **1995**, *7*, 1265–75.
- (18) Hubert-Pfalzgraf, L. G. *Inorg. Chem. Commun.* **2003**, *6*, 102–120.

stated that the catalytic activity of monoclinic BiVO_4 generated by wet chemical approaches is superior to samples of the oxide produced by solid-state techniques.^{19,20} It has been observed that the use of such soft chemical approaches to the formation of oxides can allow for the isolation of kinetic or metastable phases that are difficult to produce by more traditional techniques.¹⁷ The limitation of the wet chemical approach to the synthesis of oxides is the deliberate design and synthesis of single-source precursors whose overall stoichiometry is reflective of the target oxide that will be produced on decomposition,²¹ allowing for the formation of high purity materials at relatively low temperatures.²²

Clearly the success of this method is dependent upon the ability to efficiently produce molecular complexes with compositions representative of the desired materials and whose physical properties are compatible with the constraints of a given reaction system.²³ In comparison to the other main group metals, the coordination chemistry of bismuth is poorly developed. The difficulties encountered in exploring the coordination chemistry of the metal stem largely from the high ligand lability and Lewis acidity, coupled with the ability of the bismuth center to expand its coordination sphere readily.²⁴ These characteristics tend to result in the formation of intractable coordination oligomers or polymers that are difficult to characterize. Additionally, many known molecular bismuth complexes, which could serve as sources for the formation of heterobimetallic coordination complexes, are reported to be stubbornly unreactive under many of the conditions that are commonly employed for the synthesis of heterobimetallic systems, necessitating the development of alternate synthetic routes.²⁵ As a result, relatively few molecular heterobimetallic coordination complexes of bismuth have been reported.

The numerous potential applications of bismuth-based materials, combined with the lack of general synthetic approaches to heterobimetallic or multimetallic coordination complexes based on the metal, clearly warrant the further exploration and development of wet chemical approaches to such materials. As part of our ongoing research into developing the coordination chemistry of bismuth, we have explored the direct solubilization of polymeric bismuth salicylate by titanium isopropoxide, and wish to report here the synthesis and characterization of the new complexes $\text{BiTi}_4(\text{sal})_6(\mu\text{-O}^i\text{Pr})_3(\text{O}^i\text{Pr})_4$ (**1**), $\text{Bi}_4\text{Ti}_4(\text{sal})_{10}(\mu\text{-O}^i\text{Pr})_4(\text{O}^i\text{Pr})_4$ (**2**), and $\text{Bi}_8\text{Ti}_8(\text{sal})_{20}(\mu\text{-O}^i\text{Pr})_8(\text{O}^i\text{Pr})_8$ (**3**). The composition and structure of the compounds, as determined by single-crystal X-ray diffraction studies, provides insight into the

formation of heterometallic bismuth coordination complexes. The reactivity of these complexes provides important clues about the solution state structure of bismuth(III) salicylate.

Experimental Section

All synthetic reactions were carried out using standard Schlenk or glovebox techniques under an atmosphere of purified nitrogen or argon. Solvents were purified over an appropriate drying reagent under argon and were distilled immediately prior to use.²⁶ The starting materials triphenylbismuth (Strem Chemical Co.), titanium(IV) isopropoxide (Strem Chemical Co.), and salicylic acid (Aldrich Chemical Co.) were purchased and used as received. Bismuth(III) salicylate was prepared in situ by reacting triphenylbismuth with salicylic acid in refluxing toluene, as previously reported.²⁷ This complex was not isolated prior to reaction with titanium isopropoxide. Galbraith Laboratories performed all elemental analyses. Multinuclear NMR studies were performed on Bruker 500 and 400 MHz Avance instruments and are referenced to the protio impurity in the deuterated solvent (^1H), or to the solvent signal (^{13}C). Chemical shifts are reported in parts per million (ppm), while coupling constants are reported in hertz (Hz). Infrared spectra were collected on a Thermo-Nicolet 630 instrument utilizing an attenuated total reflectance (ATR) aperture fitted with a germanium window.

$\text{BiTi}_4(\text{sal})_6(\mu\text{-O}^i\text{Pr})_3(\text{O}^i\text{Pr})_4$ (1**) and $\text{Bi}_4\text{Ti}_4(\text{sal})_{10}(\mu\text{-O}^i\text{Pr})_4(\text{O}^i\text{Pr})_4$ (**2**). Method 1.** A toluene suspension of $[\text{Bi}(\text{Hsal})_3]_n$ (ca. 0.67 g, 1.0 mmol) was treated with neat $\text{Ti}(\text{O}^i\text{Pr})_4$ (0.6 mL, 2.0 mmol) at room temperature. The solid $[\text{Bi}(\text{Hsal})_3]_n$ rapidly dissolved, giving a clear, bright yellow solution. The solution was stirred overnight, and then, the solvent was removed under reduced pressure to give a yellow, slightly oily residue that was extracted with dichloromethane (15 mL), filtered through Celite, and layered with hexane (75 mL). Solvent diffusion was allowed to occur at $-20\text{ }^\circ\text{C}$. A small amount of compound **2** (ca. 10 mg) crystallizes after 3–4 weeks as yellow blocks. Concentration of the mother liquor to approximately 15 mL followed by layering with additional hexane (75 mL) resulted in the crystallization of **1** as bright yellow needles of the hexane solvate after an additional 2 weeks at $-20\text{ }^\circ\text{C}$. Samples of **2** prepared in this fashion were always contaminated with small amounts of **1**, precluding meaningful spectroscopic analyses of **2**. Yield of **1**: 225 mg (0.134 mmol, 27% based on Ti). ^1H NMR (C_6D_6 , 400 MHz, $25\text{ }^\circ\text{C}$): δ 0.761 (d, $J_{\text{H-H}} = 6.33$ Hz, CH_3), 0.863 (d, $J_{\text{H-H}} = 6.14$ Hz, CH_3), 0.938 (d, $J_{\text{H-H}} = 4.32$ Hz, CH_3), 1.211 (d, $J_{\text{H-H}} = 6.13$ Hz, CH_3), 1.228 (d, $J_{\text{H-H}} = 2.37$ Hz, CH_3), 1.371 (d, $J_{\text{H-H}} = 6.19$ Hz, CH_3), 1.399 (d, $J_{\text{H-H}} = 6.18$ Hz, CH_3), 1.418 (d, $J_{\text{H-H}} = 6.31$ Hz, CH_3), 1.461 (d, $J_{\text{H-H}} = 6.19$ Hz, CH_3), 1.515 (d, $J_{\text{H-H}} = 6.17$ Hz, CH_3), 1.718 (d, $J_{\text{H-H}} = 6.25$ Hz, CH_3), 1.181 (d, $J_{\text{H-H}} = 6.14$ Hz, CH_3), 1.840 (m, $J_{\text{H-H}} = 6.24$ Hz, CH_3), 4.411 (septet, $J_{\text{H-H}} = 6.22$ Hz, CH), 4.942 (septet, $J_{\text{H-H}} = 6.17$ Hz, CH), 5.280 (septet, $J_{\text{H-H}} = 6.18$ Hz, CH), 6.050 (septet, $J_{\text{H-H}} = 6.27$ Hz, CH), 6.20–8.62 (mult, ArH). $^{13}\text{C}\{^1\text{H}\}$ NMR (C_6D_6 , 125 MHz, $25\text{ }^\circ\text{C}$): δ 24.57, 24.72, 24.79, 24.88, 24.94, 25.01, 25.04, 25.57, 25.78, 26.79, 26.95, 75.37, 80.03, 80.96, 83.35, 83.43, 83.46, 84.02, 117.74, 117.88, 118.05, 118.45, 118.81, 118.89, 118.99, 119.10, 119.20, 119.42, 119.66, 119.81, 120.28, 120.49, 120.63, 120.78, 126.03, 127.87, 128.06, 128.20, 128.30, 128.39, 128.49, 128.58, 128.90, 129.21, 129.30, 129.67, 131.65, 131.77, 132.10, 132.62, 132.89, 132.89, 134.55, 135.23, 135.97, 136.14, 136.32, 136.36, 136.59, 136.85, 165.54, 167.10, 168.42, 169.48, 173.61, 174.38, 175.34, 176.00. ATR FT-IR (Ge,

(19) Tokunaga, S.; Kato, H.; Kudo, A. *Chem. Mater.* **2001**, *13*, 4624–4628.

(20) Kohtani, S.; Makino, S.; Kudo, A.; Tokumura, K.; Ishigaki, Y.; Matsunaga, T.; Nikaido, O.; Hayakawa, K.; Nakagaki, R. *Chem. Lett.* **2002**, *7*, 660–661.

(21) Kessler, V. G. *Chem. Commun.* **2003**, 1213–1222.

(22) Veith, M. J. *Chem. Soc., Dalton Trans.* **2002**, 2405–2412.

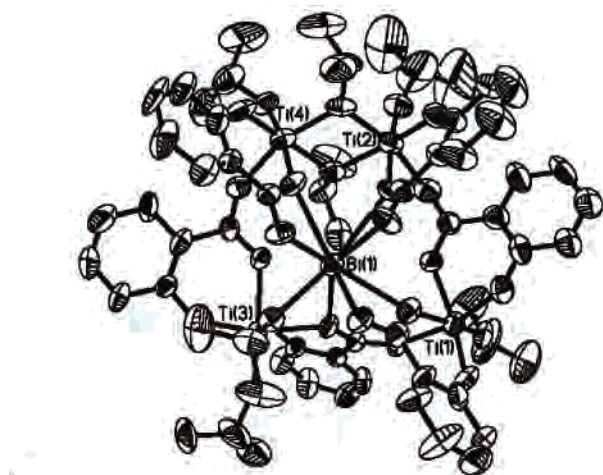
(23) Boulmaaz, S.; Papiernik, R.; Hubert-Pfalzgraf, L. G.; Septe, B.; Vaisermann, J. J. *Mater. Chem.* **1997**, *7*, 2053–2061.

(24) Briand, G. G.; Burford, N.; Cameron, T. S. *J. Chem. Soc., Chem. Commun.* **2000**, 13–14.

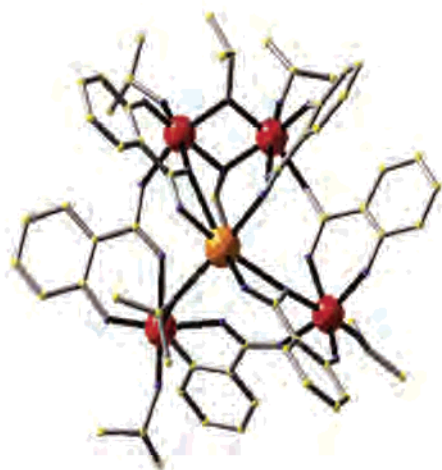
(25) Parola, S.; Papiernik, R.; Hubert-Pfalzgraf, L. G.; Jagner, S.; Hakanson, M. J. *Chem. Soc., Dalton Trans.* **1997**, 4631.

(26) Armarego, W. L. F.; Chai, C. L. L. *Purification of Laboratory Chemicals*, 5th ed.; Butterworth-Heinemann: Boston, 2003.

(27) Thurston, J. H.; Whitmire, K. H. *Inorg. Chem.* **2002**, *41*, 4194–4205.



A



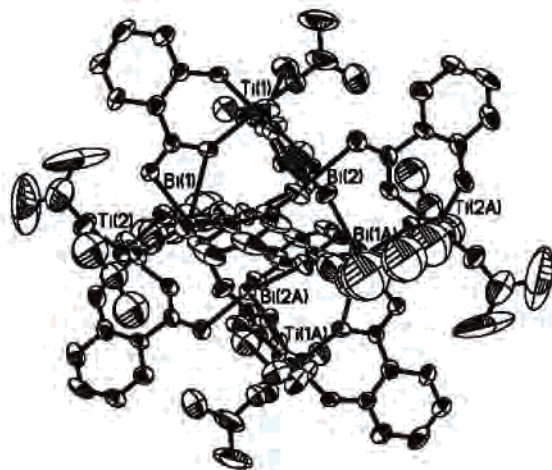
B

Figure 1. Solid-state structure of **1**. (A) ORTEP representation. Thermal ellipsoids are drawn at the 30% probability level. Hydrogen atoms have been omitted for clarity. (B) WinRay representation. Metal atoms have been emphasized to illustrate the connectivity of the complex. Hydrogen atoms have been omitted for clarity. The color scheme used is the following: Bi, orange; Ti, red; O, blue; C, yellow.

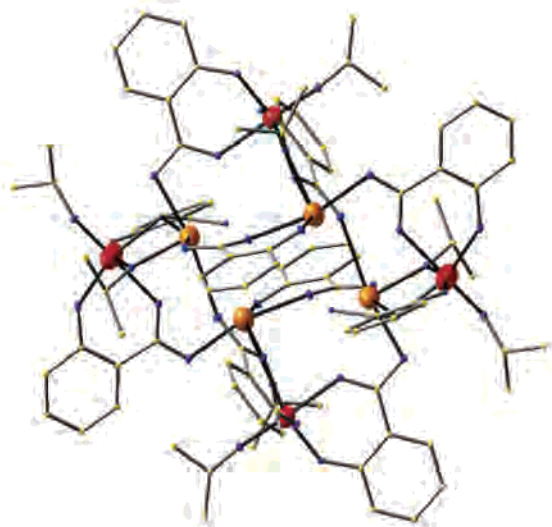
cm^{-1} : 1600, 1574, 1532, 1517, 1487, 1472, 1456, 1385, 1320, 1252, 1239, 1163, 1146, 1121, 1009, 916, 897, 859, 830, 813, 758, 702. Elemental Analysis (% Calcd for $\text{BiTi}_4\text{C}_{63}\text{H}_{73}\text{O}_{25}$): C, 46.23 (46.40); H, 4.89 (4.51).

$\text{BiTi}_4(\text{sal})_6(\mu\text{-O}^i\text{Pr})_3(\text{O}^i\text{Pr})_4$ (1**). Method 2.** A mixture of triphenylbismuth (0.44 g, 1.0 mmol) and salicylic acid (0.83 g, 6.0 mmol) was refluxed in 25 mL of toluene for 1 h. The resulting yellow paste was treated with $\text{Ti}(\text{O}^i\text{Pr})_4$ (1.2 mL, 4 mmol) dropwise. The solid was rapidly consumed, and the resulting clear, bright yellow solution was stirred at room temperature for 15 h. The reaction mixture was then concentrated to approximately 10 mL, and hexanes (25 mL) were added. The solution was mixed to give a single phase and then stored at -20°C for 15 h. During this time, yellow needle-shaped crystals deposited in the flask. Yield of **1**: 1.32 g (0.85 mmol, 85%). The product of this synthesis gave spectroscopic data (^1H NMR and FT-IR) identical to that listed for method 1.

$\text{Bi}_8\text{Ti}_8(\text{sal})_{20}(\mu\text{-O}^i\text{Pr})_8(\text{O}^i\text{Pr})_8$ (3**).** After removal of **1** from the mother liquor, as described in method 1, the filtrate was further concentrated, layered with hexane (100 mL), and allowed to recrystallize at room temperature for approximately 2 months. During this time, a few very well formed rhombohedral crystals of



A



B

Figure 2. Solid-state structure of **2**. (A) ORTEP representation. Thermal ellipsoids are drawn at the 30% probability level. Hydrogen atoms have been omitted for clarity. (B) WinRay representation of the solid-state structure of **2**. Metal atoms have been emphasized to illustrate the connectivity of the complex. Hydrogen atoms have been omitted for clarity. The color scheme used is the following: Bi, orange; Ti, red; O, blue; C, yellow.

3 deposited in the flask in addition to crystals of **1**. Samples of **3** were separated under a microscope and characterized crystallographically.

Crystal Structure Determination. Compounds **1–3** were studied on a Bruker Smart 1000 diffractometer equipped with a CCD area detector. The data were corrected for Lorentz and polarization effects. Absorption correction was applied using the program SADABS.²⁸ The structures were solved using either direct methods (**1** and **3**) or from the Patterson map (**2**) with the SHELXTL software package to locate the heavy atoms.²⁹ All other atoms were identified by successive Fourier difference maps and refined using the full-matrix least-squares technique on F^2 . All non-hydrogen atoms, with the exceptions discussed below, were refined anisotropically. Hydrogen atoms in all of the complexes were placed

(28) Sheldrick, G. *SADABS*, 5.1; University of Göttingen: Göttingen, Germany, 1997.

(29) Sheldrick, G. *SHELXTL*, 6.1; University of Göttingen: Göttingen, Germany, 2001.

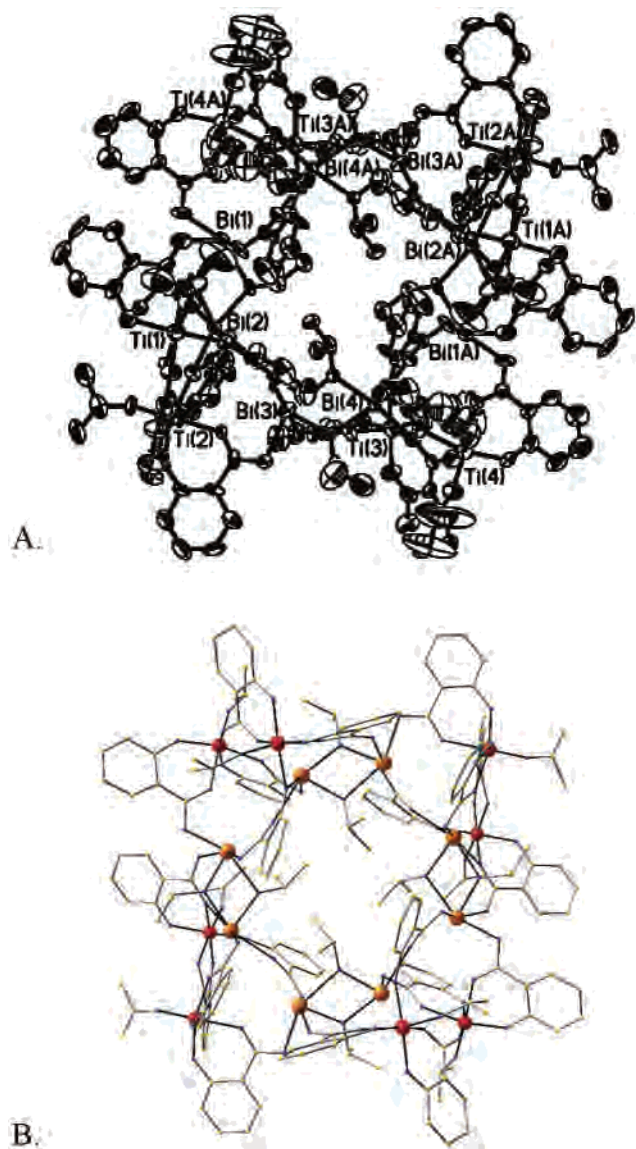


Figure 3. Solid-state structure of **3**. (A) ORTEP representation. Thermal ellipsoids are drawn at the 30% probability level. Hydrogen atoms have been omitted for clarity. (B) WinRay representation of the solid-state structure of **3**. Metal atoms have been emphasized to illustrate the connectivity of the complex. Hydrogen atoms have been omitted for clarity. The color scheme used is the following: Bi, orange; Ti, red; O, blue; C, yellow.

in calculated positions and allowed to ride on the adjacent atom. Hydrogen atoms associated with phenolic oxygen atoms were placed in calculated positions and refined geometrically using a riding model. Under the conditions employed in these experiments, all of the complexes cocrystallize with a significant amount of lattice solvent including hexane, dichloromethane or toluene (depending on which solvent was used for crystallization), and 2-propanol. In the case of compound **2**, this resulted in rapid efflorescence of the sample and inevitable crystal decay, even at reduced temperatures. The data presented here allow for the unequivocal identification of the solid-state structure of the complex, but the refined structure is of limited quality. Repeated attempts to achieve higher quality data were not successful. For compounds **2** and **3**, the bond distances and angles of the isopropoxide ligands showed distortion from normal sp^3 hybridized carbon, and so, the isopropoxide ligands were refined with constraints to give them more chemically reasonable geometries. In the case of **3**, two of the isopropoxide ligands showed

Table 1. Crystallographic Data for Compounds **1–3**

	1	2	3
formula	$\text{BiTi}_4\text{C}_6\text{H}_7\text{O}_{25}$	$\text{Bi}_4\text{Ti}_4\text{C}_{94}\text{H}_{96}\text{O}_{38}$	$\text{Bi}_8\text{Ti}_8\text{C}_{188}\text{H}_{192}\text{O}_{76}$
fw	1630.79	2861.22	5722.46
space group	$P\bar{1}$	$P\bar{1}$	$C2/c$
Z	2	1	8
cryst syst	triclinic	triclinic	monoclinic
a (Å)	12.130(2)	13.551(3)	24.115(5)
b (Å)	15.073(3)	14.397(3)	29.755(6)
c (Å)	23.789(5)	16.376(3)	35.369(7)
α (deg)	98.62(3)	66.70(3)	
β (deg)	101.38(3)	76.71(3)	108.59(3)
γ (deg)	113.55(3)	79.71(3)	
V , Å ³	3779.9(13)	2841.9(10)	24055(8)
D (calc), $\text{g}\cdot\text{cm}^{-3}$	1.433	1.672	1.580
temp (°C)	25	−60	25
λ , Mo K α (Å)	0.71073	0.71073	0.71073
μ (cm^{-1})	27.95	65.10	61.53
$R1^a$	0.0723	0.0460	0.0390
$wR2^b$	0.2166	0.1374	0.0786

^a Conventional R on F_{hkl} : $\sum|F_o| - |F_c|/\sum|F_o|$. ^b Conventional R on $|F_{hkl}|^2$: $\{\sum w|F_o^2 - F_c^2|/\sum w(F_o^2)\}^{1/2}$.

disorder that was successfully modeled. For the other isopropoxide ligands, the apparent disorder could not be resolved. The structures of complexes **2** and **3** were also probed using the program PLATON and were found to contain void areas of 503.5 Å³/unit cell and 6632.3 Å³/unit cell, respectively, corresponding to the presence of approximately 1.5 and 2.5 molecules of solvent per asymmetric unit of the heterobimetallic complex.³⁰ This lattice solvent could not be located with any certainty from Fourier maps of the residual electron density of the X-ray data, and it was clear that the solvent is highly disordered in the crystal lattices of both complexes. Consequently, the electron density of the disordered solvent was subtracted from the data using the program SQUEEZE.³⁰ The crystal structures are found in Figures 1–3. Due to the structural complexity of **2** and **3**, WinRay representations have been employed for clarity.³¹

Results and Discussion

The oligomeric complex produced from the reaction of a 1:3 mixture of triphenyl bismuth and salicylic acid can be readily solubilized by reaction with titanium isopropoxide. Under the conditions employed in our study (i.e. 25 °C, toluene), 2 equiv of the metal alkoxide were required to achieve complete dissolution of the bismuth salicylate. Subsequent analysis of the solution produced from this reaction indicated that it contained a mixture of complexes that were separable from one another by fractional crystallization. The products of the reaction were characterized by single crystal X-ray diffraction studies and, in the case of the high yield product **1**, by spectroscopic techniques.

The solid-state structures of the new complexes, as determined by single crystal X-ray diffraction, are presented in Figures 1–3, while pertinent details relating to data collection and structure refinement are presented in Tables 1–4. Complex **1**, which is the major product of the reaction, consists of a central bismuth atom that caps a ring of four titanium atoms. The bismuth atom is eight-coordinate and

(30) Spek, A. L. *Platon, A Multipurpose Crystallographic Tool*; Utrecht University: Utrecht, The Netherlands, 2001.

(31) Solttek, R. *Winray*, GL; Heidelberg University: Heidelberg, Germany, 2000.

Table 2. Selected Bond Lengths [Å] and Angles [deg] for **1**

Bi(1)–O(23)	2.276(9)	Ti(4)–O(111)	2.000(10)
Bi(1)–O(33)	2.316(9)	Ti(4)–O(43)	2.012(11)
Bi(1)–O(71)	2.326(9)	Ti(4)–O(101)	2.027(9)
Bi(1)–O(13)	2.401(9)	Ti(4)–O(32)	2.093(10)
Bi(1)–O(22)	2.534(9)	O(23)–Bi(1)–O(33)	89.3(3)
Bi(1)–O(32)	2.545(9)	O(23)–Bi(1)–O(71)	78.3(3)
Bi(1)–O(52)	2.692(9)	O(33)–Bi(1)–O(71)	78.0(3)
Bi(1)–O(12)	2.715(9)	O(23)–Bi(1)–O(13)	74.1(3)
Bi(1)–Ti(3)	3.510(3)	O(33)–Bi(1)–O(13)	76.7(3)
Ti(1)–O(91)	1.738(9)	O(71)–Bi(1)–O(13)	142.5(3)
Ti(1)–O(21)	1.893(10)	O(23)–Bi(1)–O(22)	53.2(3)
Ti(1)–O(61)	1.896(11)	O(33)–Bi(1)–O(22)	138.5(3)
Ti(1)–O(53)	2.029(9)	O(71)–Bi(1)–O(22)	106.6(3)
Ti(1)–O(62)	2.044(10)	O(13)–Bi(1)–O(22)	76.2(3)
Ti(1)–O(22)	2.116(10)	O(23)–Bi(1)–O(32)	138.5(3)
Ti(2)–O(131)	1.747(9)	O(33)–Bi(1)–O(32)	53.2(3)
Ti(2)–O(11)	1.873(10)	O(71)–Bi(1)–O(32)	106.1(3)
Ti(2)–O(63)	1.989(10)	O(13)–Bi(1)–O(32)	79.8(3)
Ti(2)–O(101)	2.015(9)	O(22)–Bi(1)–O(32)	147.2(3)
Ti(2)–O(111)	2.028(9)	O(23)–Bi(1)–O(52)	92.8(3)
Ti(2)–O(12)	2.072(10)	O(33)–Bi(1)–O(52)	137.4(3)
Ti(2)–Ti(4)	3.187(4)	O(71)–Bi(1)–O(52)	60.9(3)
Ti(3)–O(81)	1.743(9)	O(13)–Bi(1)–O(52)	144.2(3)
Ti(3)–O(41)	1.864(9)	O(22)–Bi(1)–O(52)	69.5(3)
Ti(3)–O(51)	1.880(9)	O(32)–Bi(1)–O(52)	126.0(3)
Ti(3)–O(71)	1.998(9)	O(23)–Bi(1)–O(12)	116.5(3)
Ti(3)–O(52)	2.102(9)	O(33)–Bi(1)–O(12)	101.8(3)
Ti(3)–O(42)	2.148(10)	O(71)–Bi(1)–O(12)	165.2(3)
Ti(4)–O(121)	1.759(8)	O(13)–Bi(1)–O(12)	49.6(3)
Ti(4)–O(31)	1.889(11)	O(22)–Bi(1)–O(12)	83.5(3)
O(32)–Bi(1)–O(12)	63.9(3)	O(111)–Ti(2)–O(12)	87.1(4)
O(52)–Bi(1)–O(12)	114.9(3)	O(81)–Ti(3)–O(41)	95.5(4)
O(91)–Ti(1)–O(21)	100.7(5)	O(81)–Ti(3)–O(51)	96.4(4)
O(91)–Ti(1)–O(61)	96.5(5)	O(41)–Ti(3)–O(51)	97.3(4)
O(21)–Ti(1)–O(61)	94.1(5)	O(81)–Ti(3)–O(71)	101.1(4)
O(91)–Ti(1)–O(53)	89.7(4)	O(41)–Ti(3)–O(71)	99.6(4)
O(21)–Ti(1)–O(53)	96.9(4)	O(51)–Ti(3)–O(71)	154.3(4)
O(61)–Ti(1)–O(53)	166.2(4)	O(81)–Ti(3)–O(52)	97.7(4)
O(91)–Ti(1)–O(62)	97.2(4)	O(41)–Ti(3)–O(52)	166.8(4)
O(21)–Ti(1)–O(62)	162.0(4)	O(51)–Ti(3)–O(52)	81.8(4)
O(61)–Ti(1)–O(62)	83.3(4)	O(71)–Ti(3)–O(52)	77.4(3)
O(53)–Ti(1)–O(62)	83.7(4)	O(81)–Ti(3)–O(42)	178.1(4)
O(91)–Ti(1)–O(22)	173.1(4)	O(41)–Ti(3)–O(42)	82.7(4)
O(21)–Ti(1)–O(22)	81.4(4)	O(51)–Ti(3)–O(42)	84.6(4)
O(61)–Ti(1)–O(22)	89.8(4)	O(71)–Ti(3)–O(42)	78.5(3)
O(53)–Ti(1)–O(22)	83.5(4)	O(52)–Ti(3)–O(42)	84.1(3)
O(62)–Ti(1)–O(22)	80.8(4)	O(121)–Ti(4)–O(31)	91.3(5)
O(131)–Ti(2)–O(11)	93.8(5)	O(121)–Ti(4)–O(111)	101.1(4)
O(131)–Ti(2)–O(63)	94.4(5)	O(31)–Ti(4)–O(111)	98.5(4)
O(11)–Ti(2)–O(63)	97.7(5)	O(121)–Ti(4)–O(43)	92.9(4)
O(131)–Ti(2)–O(101)	100.1(4)	O(31)–Ti(4)–O(43)	92.4(4)
O(11)–Ti(2)–O(101)	161.6(4)	O(111)–Ti(4)–O(43)	161.9(4)
O(63)–Ti(2)–O(101)	93.3(4)	O(121)–Ti(4)–O(101)	98.9(4)
O(131)–Ti(2)–O(111)	97.9(4)	O(31)–Ti(4)–O(101)	169.1(4)
O(11)–Ti(2)–O(111)	90.9(4)	O(111)–Ti(4)–O(101)	75.7(4)
O(63)–Ti(2)–O(111)	164.5(4)	O(43)–Ti(4)–O(101)	91.0(4)
O(101)–Ti(2)–O(111)	75.4(4)	O(121)–Ti(4)–O(32)	169.8(4)
O(131)–Ti(2)–O(12)	173.7(5)	O(31)–Ti(4)–O(32)	80.9(4)
O(11)–Ti(2)–O(12)	82.2(4)	O(111)–Ti(4)–O(32)	86.6(4)
O(63)–Ti(2)–O(12)	81.4(4)	O(43)–Ti(4)–O(32)	81.0(4)
O(101)–Ti(2)–O(12)	84.9(3)	O(101)–Ti(4)–O(32)	89.4(3)
Ti(1)–O(22)–Bi(1)	134.7(4)	Ti(3)–O(71)–Bi(1)	108.3(3)
Ti(4)–O(32)–Bi(1)	132.0(4)	Ti(2)–O(101)–Ti(4)	104.1(4)
Ti(3)–O(52)–Bi(1)	93.3(3)	Ti(4)–O(111)–Ti(2)	104.6(4)

adopts a roughly square prismatic geometry. All of the titanium atoms exist in distorted octahedral coordination environments in which there are two long, two intermediate, and two short Ti–O distances with the long distances being trans to the shortest ones. The Bi–O bond distances range from 2.276(9) to 2.715(9) Å. The solid-state structure of **1** is reminiscent of the complexes BiM₄(μ-O)₄(sal)₄(Hsal)₃-

Table 3. Selected Bond Lengths [Å] and Angles [deg] for **2^a**

Bi(1)–O(81)	2.186(6)	O(81)–Bi(1)–O(52)	67.5(3)
Bi(1)–O(13)	2.273(6)	O(13)–Bi(1)–O(52)	80.4(3)
Bi(1)–O(52)	2.390(8)	O(81)–Bi(1)–O(33)	92.3(2)
Bi(1)–O(33)	2.366(7)	O(13)–Bi(1)–O(33)	79.7(3)
Bi(1)–O(43)	2.606(6)	O(52)–Bi(1)–O(33)	152.4(3)
Bi(1)–O(12)	2.679(5)	O(81)–Bi(1)–O(43)	86.5(2)
Bi(1)–O(32)	2.690(6)	O(13)–Bi(1)–O(43)	158.8(3)
Bi(2)–O(31)	2.127(6)	O(52)–Bi(1)–O(43)	114.8(2)
Bi(2)–O(91)	2.194(5)	O(33)–Bi(1)–O(43)	80.8(2)
Bi(2)–O(32)	2.320(6)	O(81)–Bi(1)–O(12)	137.1(2)
Bi(2)–O(23)	2.328(6)	O(13)–Bi(1)–O(12)	51.6(2)
Bi(2)–O(42)#1	2.517(6)	O(52)–Bi(1)–O(12)	94.3(2)
Ti(1)–O(61)	1.759(6)	O(33)–Bi(1)–O(12)	88.1(2)
Ti(1)–O(11)	1.872(6)	O(43)–Bi(1)–O(12)	135.7(2)
Ti(1)–O(41)#1	1.885(6)	O(81)–Bi(1)–O(32)	138.1(2)
Ti(1)–O(42)#1	2.045(6)	O(13)–Bi(1)–O(32)	102.1(2)
Ti(1)–O(91)	2.085(6)	O(52)–Bi(1)–O(32)	154.1(2)
Ti(1)–O(12)	2.142(6)	O(33)–Bi(1)–O(32)	50.5(2)
Ti(2)–O(71)	1.742(7)	O(43)–Bi(1)–O(32)	71.0(2)
Ti(2)–O(21)#1	1.884(7)	O(12)–Bi(1)–O(32)	68.95(19)
Ti(2)–O(51)	1.850(9)	O(31)–Bi(2)–O(91)	90.3(2)
Ti(2)–O(81)	2.078(7)	O(31)–Bi(2)–O(32)	79.2(2)
Ti(2)–O(52)	2.025(8)	O(91)–Bi(2)–O(32)	83.5(2)
Ti(2)–O(22)#1	2.148(6)	O(31)–Bi(2)–O(23)	87.6(2)
O(21)–Ti(2)#1	1.884(7)	O(91)–Bi(2)–O(23)	81.4(2)
O(22)–Ti(2)#1	2.148(6)	O(32)–Bi(2)–O(23)	159.8(2)
O(41)–Ti(1)#1	1.885(6)	O(31)–Bi(2)–O(42)#1	150.0(2)
O(42)–Ti(1)#1	2.045(6)	O(91)–Bi(2)–O(42)#1	65.26(19)
O(42)–Bi(2)#1	2.517(6)	O(32)–Bi(2)–O(42)#1	81.0(2)
O(81)–Bi(1)–O(13)	86.3(2)	O(23)–Bi(2)–O(42)#1	104.5(2)
O(61)–Ti(1)–O(11)	99.7(3)	O(71)–Ti(2)–O(81)	92.8(4)
O(61)–Ti(1)–O(41)#1	95.2(3)	O(21)#1–Ti(2)–O(81)	95.9(3)
O(11)–Ti(1)–O(41)#1	97.4(3)	O(51)–Ti(2)–O(81)	161.9(3)
O(61)–Ti(1)–O(42)#1	97.5(3)	O(71)–Ti(2)–O(52)	99.9(3)
O(11)–Ti(1)–O(42)#1	162.7(3)	O(21)#1–Ti(2)–O(52)	162.7(3)
O(41)#1–Ti(1)–O(42)#1	83.4(3)	O(51)–Ti(2)–O(52)	87.1(4)
O(61)–Ti(1)–O(91)	93.6(3)	O(81)–Ti(2)–O(52)	76.7(3)
O(11)–Ti(1)–O(91)	99.9(2)	O(71)–Ti(2)–O(22)#1	176.2(4)
O(41)#1–Ti(1)–O(91)	158.9(3)	O(21)#1–Ti(2)–O(22)#1	83.1(3)
O(42)#1–Ti(1)–O(91)	76.4(2)	O(51)–Ti(2)–O(22)#1	85.9(4)
O(61)–Ti(1)–O(12)	177.9(3)	O(81)–Ti(2)–O(22)#1	83.6(3)
O(11)–Ti(1)–O(12)	81.9(2)	O(52)–Ti(2)–O(22)#1	80.6(3)
O(41)#1–Ti(1)–O(12)	85.8(3)	Ti(1)–O(12)–Bi(1)	142.1(3)
O(42)#1–Ti(1)–O(12)	80.8(2)	Bi(2)–O(32)–Bi(1)	136.7(3)
O(91)–Ti(1)–O(12)	84.8(2)	Ti(1)#1–O(42)–Bi(2)#1	103.7(2)
O(71)–Ti(2)–O(21)#1	96.0(3)	Ti(2)–O(52)–Bi(1)	104.4(3)
O(71)–Ti(2)–O(51)	97.9(4)	Ti(2)–O(81)–Bi(1)	110.1(3)
O(21)#1–Ti(2)–O(51)	97.4(4)	Ti(1)–O(91)–Bi(2)	114.5(2)

^a Symmetry transformations used to generate equivalent atoms: #1 $-x + 1, -y + 1, -z + 1$.

(OPrⁱ)₄ (M = Nb, Ta), which show M₄O₄ squares capped on one side by a bismuth salicylate moiety.³²

The solution-state behavior of compound **1** was investigated through multinuclear NMR experiments. Figures 4 and 5 show the methyne region, methyl region, and 2D COSY ¹H NMR spectra.³³ From Figure 4A, four methyne multiplets that integrated as 1:3:2:1 were identified. The methyl region of the spectrum (Figure 4B) is complex, indicating that the methyl groups of the isopropoxides were inequivalent and therefore diastereotopic. The methyne signals with intensities 3 and 2 clearly arise from close overlap of independent signals. This overlap was confirmed by the 2D COSY spectrum, which shows relationships between the seven different methyne signals and the 14 different methyl groups (see Figure 5), consistent with the solid-state structure of **1**. The aromatic region of the spectrum is also consistent with

(32) Thurston, J. H.; Whitmire, K. H. *Inorg. Chem.* **2003**, *42*, 2014–2023.

(33) Gottlieb, H. E.; Kotlyar, V.; Nudelman, A. *J. Org. Chem.* **1997**, *62*, 7512–7515.

Table 4. Selected Bond Lengths [Å] and Angles [deg] for **3**^a

Bi(1)–O(61)	2.113(5)	Ti(4)–O(132)	2.041(7)	O(21)–Bi(4)–O(133)	88.1(2)	O(163)–Ti(2)–O(172)	83.3(2)
Bi(1)–O(103)#1	2.241(7)	Ti(4)–O(192)	2.131(7)	O(21)–Bi(4)–O(102)	92.6(2)	O(51)–Ti(2)–O(112)	173.8(3)
Bi(1)–O(193)#1	2.290(7)	O(103)–Bi(1)#1	2.241(7)	O(133)–Bi(4)–O(102)	75.1(2)	O(171)–Ti(2)–O(112)	85.2(3)
Bi(1)–O(61)	2.394(6)	O(193)–Bi(1)#1	2.290(7)	O(21)–Bi(4)–O(31)	71.5(2)	O(111)–Ti(2)–O(112)	83.5(3)
Bi(1)–O(123)	2.443(7)	O(61)–Bi(1)–O(103)#1	81.9(2)	O(133)–Bi(4)–O(31)	78.3(2)	O(163)–Ti(2)–O(112)	81.5(3)
Bi(2)–O(71)	2.144(5)	O(61)–Bi(1)–O(193)#1	84.5(2)	O(102)–Bi(4)–O(31)	149.4(2)	O(172)–Ti(2)–O(112)	81.2(3)
Bi(2)–O(152)	2.305(6)	O(103)#1–Bi(1)–O(193)#1	82.7(3)	O(21)–Bi(4)–O(101)	91.5(2)	O(41)–Ti(3)–O(141)	100.2(3)
Bi(2)–O(61)	2.350(6)	O(61)–Bi(1)–O(71)	69.7(2)	O(133)–Bi(4)–O(101)	146.5(2)	O(41)–Ti(3)–O(181)	101.4(3)
Bi(2)–O(173)	2.437(6)	O(103)#1–Bi(1)–O(71)	88.7(2)	O(102)–Bi(4)–O(101)	71.4(2)	O(141)–Ti(3)–O(181)	95.1(3)
Bi(2)–O(151)	2.513(6)	O(193)#1–Bi(1)–O(71)	153.7(2)	O(31)–Bi(4)–O(101)	132.97(19)	O(41)–Ti(3)–O(101)	92.3(3)
Bi(2)–O(122)	2.573(6)	O(61)–Bi(1)–O(123)	76.3(2)	O(21)–Bi(4)–O(182)	145.7(2)	O(141)–Ti(3)–O(101)	101.3(3)
Bi(2)–O(172)	2.686(5)	O(103)#1–Bi(1)–O(123)	156.3(2)	O(133)–Bi(4)–O(182)	126.2(2)	O(181)–Ti(3)–O(101)	156.4(3)
Bi(3)–O(31)	2.104(6)	O(193)#1–Bi(1)–O(123)	86.2(2)	O(102)–Bi(4)–O(182)	96.1(2)	O(41)–Ti(3)–O(182)	92.5(3)
Bi(3)–O(113)	2.276(6)	O(71)–Bi(1)–O(123)	92.2(2)	O(31)–Bi(4)–O(182)	111.80(19)	O(141)–Ti(3)–O(182)	167.3(3)
Bi(3)–O(153)	2.299(6)	O(71)–Bi(2)–O(152)	87.0(2)	O(101)–Bi(4)–O(182)	60.5(2)	O(181)–Ti(3)–O(182)	82.6(3)
Bi(3)–O(143)	2.367(6)	O(71)–Bi(2)–O(61)	70.1(2)	O(21)–Bi(4)–O(142)	85.3(2)	O(101)–Ti(3)–O(182)	77.6(3)
Bi(3)–O(21)	2.455(5)	O(152)–Bi(2)–O(61)	142.9(2)	O(133)–Bi(4)–O(142)	154.14(19)	O(41)–Ti(3)–O(142)	167.3(3)
Bi(4)–O(21)	2.108(5)	O(71)–Bi(2)–O(173)	90.3(2)	O(102)–Bi(4)–O(142)	130.07(19)	O(141)–Ti(3)–O(142)	84.3(3)
Bi(4)–O(133)	2.357(6)	O(152)–Bi(2)–O(173)	73.2(2)	O(31)–Bi(4)–O(142)	75.87(18)	O(181)–Ti(3)–O(142)	89.9(3)
Bi(4)–O(102)	2.368(6)	O(61)–Bi(2)–O(173)	78.0(2)	O(101)–Bi(4)–O(142)	58.86(18)	O(101)–Ti(3)–O(142)	75.1(2)
Bi(4)–O(31)	2.378(6)	O(71)–Bi(2)–O(151)	91.7(2)	O(182)–Bi(4)–O(142)	63.8(2)	O(182)–Ti(3)–O(142)	83.2(3)
Bi(4)–O(101)	2.530(6)	O(152)–Bi(2)–O(151)	73.7(2)	O(81)–Ti(1)–O(161)	97.9(3)	O(11)–Ti(4)–O(191)	99.4(3)
Bi(4)–O(182)	2.645(7)	O(61)–Bi(2)–O(151)	133.44(19)	O(81)–Ti(1)–O(121)	98.6(3)	O(11)–Ti(4)–O(131)	94.7(4)
Bi(4)–O(142)	2.677(6)	O(173)–Bi(2)–O(151)	146.7(2)	O(161)–Ti(1)–O(121)	99.1(3)	O(191)–Ti(4)–O(131)	99.2(3)
Ti(1)–O(81)	1.751(6)	O(71)–Bi(2)–O(122)	86.1(2)	O(81)–Ti(1)–O(122)	92.5(3)	O(11)–Ti(4)–O(183)	92.1(3)
Ti(1)–O(161)	1.843(6)	O(152)–Bi(2)–O(122)	134.6(2)	O(161)–Ti(1)–O(122)	169.2(3)	O(191)–Ti(4)–O(183)	89.8(3)
Ti(1)–O(121)	1.880(7)	O(61)–Bi(2)–O(122)	74.2(2)	O(121)–Ti(1)–O(122)	82.4(3)	O(131)–Ti(4)–O(183)	167.6(3)
Ti(1)–O(122)	2.058(6)	O(173)–Bi(2)–O(122)	151.5(2)	O(81)–Ti(1)–O(151)	97.8(3)	O(11)–Ti(4)–O(132)	97.9(3)
Ti(1)–O(151)	2.098(6)	O(151)–Bi(2)–O(122)	61.7(2)	O(161)–Ti(1)–O(151)	97.6(3)	O(191)–Ti(4)–O(132)	162.0(3)
Ti(1)–O(162)	2.127(6)	O(71)–Bi(2)–O(172)	140.5(2)	O(121)–Ti(1)–O(151)	154.7(3)	O(131)–Ti(4)–O(132)	84.2(3)
Ti(2)–O(51)	1.734(6)	O(152)–Bi(2)–O(172)	80.63(19)	O(122)–Ti(1)–O(151)	77.8(3)	O(183)–Ti(4)–O(132)	84.6(3)
Ti(2)–O(171)	1.879(7)	O(61)–Bi(2)–O(172)	98.47(18)	O(81)–Ti(1)–O(162)	173.8(3)	O(11)–Ti(4)–O(192)	177.5(3)
Ti(2)–O(111)	1.888(7)	O(173)–Bi(2)–O(172)	50.22(19)	O(161)–Ti(1)–O(162)	84.6(3)	O(191)–Ti(4)–O(192)	83.1(3)
Ti(2)–O(163)	1.992(7)	O(151)–Bi(2)–O(172)	119.90(18)	O(121)–Ti(1)–O(162)	86.6(3)	O(131)–Ti(4)–O(192)	84.9(3)
Ti(2)–O(172)	2.036(6)	O(122)–Bi(2)–O(172)	128.35(19)	O(122)–Ti(1)–O(162)	84.8(2)	O(183)–Ti(4)–O(192)	87.8(3)
Ti(2)–O(112)	2.120(7)	O(31)–Bi(3)–O(113)	84.0(2)	O(151)–Ti(1)–O(162)	76.2(2)	O(132)–Ti(4)–O(192)	79.6(3)
Ti(3)–O(41)	1.746(6)	O(31)–Bi(3)–O(153)	78.3(2)	O(51)–Ti(2)–O(171)	100.9(3)	Bi(4)–O(21)–Bi(3)	106.7(2)
Ti(3)–O(141)	1.855(7)	O(113)–Bi(3)–O(153)	85.7(2)	O(51)–Ti(2)–O(111)	96.0(3)	Bi(1)–O(61)–Bi(2)	110.0(2)
Ti(3)–O(181)	1.888(7)	O(31)–Bi(3)–O(143)	81.2(2)	O(171)–Ti(2)–O(111)	97.7(3)	Bi(2)–O(71)–Bi(1)	107.4(2)
Ti(3)–O(101)	2.064(6)	O(113)–Bi(3)–O(143)	79.8(2)	O(51)–Ti(2)–O(163)	92.3(3)	Ti(3)–O(101)–Bi(4)	100.7(2)
Ti(3)–O(182)	2.100(7)	O(153)–Bi(3)–O(143)	156.1(2)	O(171)–Ti(2)–O(163)	162.2(3)	Ti(1)–O(122)–Bi(2)	100.0(3)
Ti(3)–O(142)	2.138(7)	O(31)–Bi(3)–O(21)	70.0(2)	O(111)–Ti(2)–O(163)	92.5(3)	Ti(3)–O(142)–Bi(4)	94.3(2)
Ti(4)–O(11)	1.731(7)	O(113)–Bi(3)–O(21)	151.8(2)	O(51)–Ti(2)–O(172)	99.0(3)	Ti(1)–O(151)–Bi(2)	100.8(3)
Ti(4)–O(191)	1.854(7)	O(153)–Bi(3)–O(21)	98.9(2)	O(171)–Ti(2)–O(172)	83.0(3)	Ti(2)–O(172)–Bi(2)	133.0(3)
Ti(4)–O(131)	1.869(8)	O(143)–Bi(3)–O(21)	85.5(2)	O(111)–Ti(2)–O(172)	164.6(3)	Ti(3)–O(182)–Bi(4)	96.1(3)
Ti(4)–O(183)	2.000(7)						

^a Symmetry transformations used to generate equivalent atoms: #1 $-x + 1, y, -z + 1/2$.

the solid-state structure of the complex since six sets of doublets indicate the presence of six unique salicylate environments (see Supporting Information). Unequivocal confirmation of the ¹H NMR analysis was obtained from ¹³C{¹H} NMR experiments which can be found in Supporting Information. These data are consistent with retention of the solid-state structure in solution, as is consistent with observations for other bismuth–titanium salicylate complexes that we have reported.^{27,32}

Compounds **2** and **3**, minor side products of the initial synthesis of **1**, are cyclic isomers. Compound **2**, which is the first compound to be isolated from the reaction mixture (method 1) by fractional crystallization, can be viewed as composed of two Bi₂Ti₂(sal)₅(μ-OⁱPr)₂(OⁱPr)₂ units (Figure 6). The four metal centers in each subunit are assembled via bridging salicylate and alkoxide interactions with one another. The overall molecule is organized so that there is a central square of bismuth atoms with the titanium atoms located on the periphery of the molecule. Each bismuth atom

interacts with the two adjacent bismuth atoms through bridging salicylate ligands, and each bismuth atom further interacts with two titanium atoms, one through the carboxylate of a salicylate ligand and the other through bridging interactions of both an alkoxide and a salicylate ligand, to form a four membered MM'OO' ring system (Figure 7).

Similar to **2**, complex **3** is composed of four Bi₂Ti₂(sal)₅-(OⁱPr)₄ subunits, which are arranged in a centrosymmetric ring structure. In this case, however, the connectivity of the individual subunits has undergone significant reorganization relative to that observed in the solid-state structure of **2**. Adjacent bismuth and titanium atoms now interact only through bridging salicylate interactions. The tetranuclear subunit can be pictured as being subdivided into bimetallic units of bismuth, and individual titaniums (Figures 8 and 9). It is observed that adjacent bismuth atoms are bridged by a salicylate and two bridging alkoxide ligands. Titanium atoms can be regarded as individual units, since each shares only one salicylate ligand with an adjacent titanium, i.e., Ti1

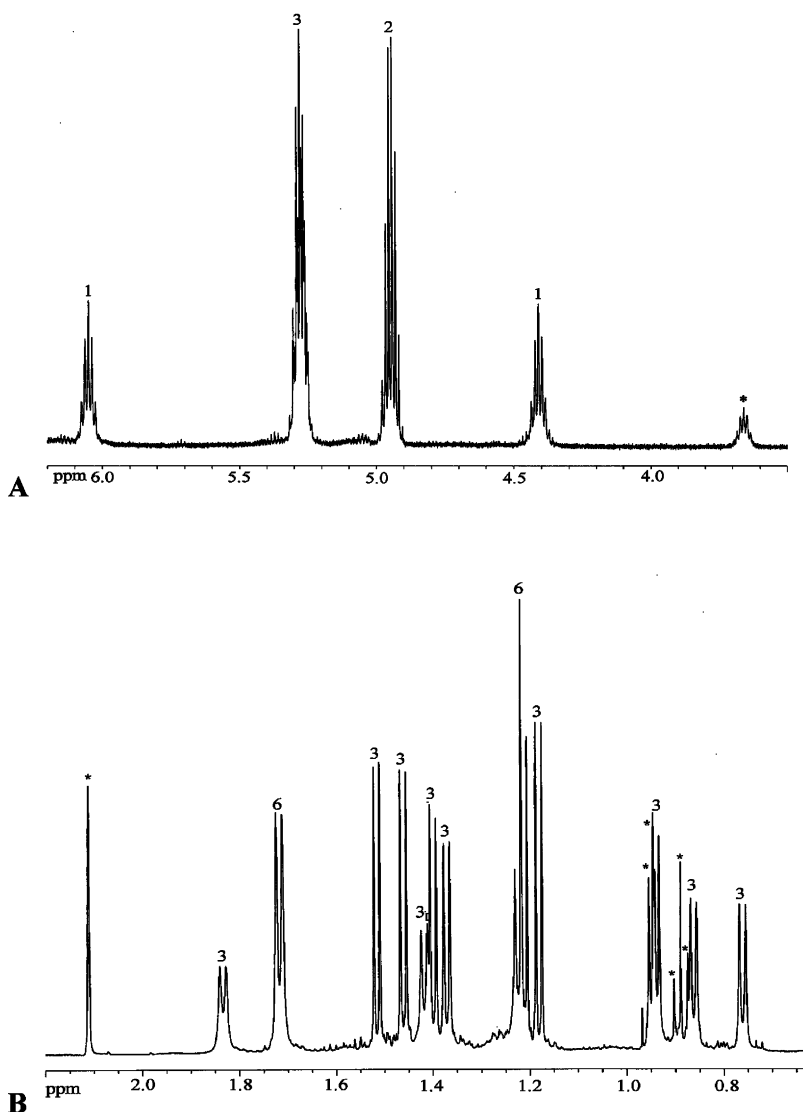


Figure 4. ^1H NMR spectrum of $\text{BiTi}_4(\text{sal})_6(\text{O}'\text{Pr})_7$ (**1**) in C_6D_6 . The relative peak intensities are indicated above each multiplet, and asterisks indicate solvent peaks. (A) Methyne region with solvent signal identified as 2-propanol at 3.67 ppm multiplet. (B) Methyl region with solvent signals identified as toluene, 2.11 ppm singlet; 2-propanol, 0.95 ppm doublet; and hexane, 0.89 ppm triplet.³³

with Ti2, and Ti3 with Ti4. An important difference between **2** and **3** is that all of the bridging alkoxide interactions occur between bismuth atoms in **3** whereas in **2** the alkoxides bridge between Ti and Bi. As with the Bi–O–Ti interaction in complex **2**, the Bi–O–Bi interaction in **3** is asymmetric, with one bond being on average 0.27 Å longer than the other, indicating that the alkoxide ligand is shared unequally between the two metal centers. This is in agreement with the observations that have been made on other bismuth alkoxide complexes including $[\text{Bi}(\text{OCH}(\text{CF}_3)_2)_3 \cdot \text{THF}]_2$.³⁴ Both **2** and **3** have large cavities in which the solvent is occluded. In the case of **2**, the solvent is primarily in a void centered at the origin (0,0,0), while the molecule is centered at $(\frac{1}{2}, \frac{1}{2}, \frac{1}{2})$. For **3** there are several smaller void areas located around the periphery of the molecule.

It is noteworthy that all of the complexes show bridging alkoxide ligands attached to bismuth. In the case of **1** and **2**,

this bridge occurs between a titanium and bismuth atom, whereas in the case of **3**, the bridging alkoxides are associated exclusively with the bismuth atoms. Only a handful of such complexes showing bridging alkoxide interactions between bismuth and another metal have been reported.^{1,3,25,35,36} Additionally, there has been no spectroscopic or crystallographic evidence for the interaction of an alkoxide ligand with a bismuth center in any of the other similar heterometallic complexes that we have produced that contain both salicylate and alkoxide ligands, the latter always previously being associated with the transition metal portion of the molecule. In this case, it seems plausible that the formation of the alkoxide interaction between the two metal species (**1** and **2**) or between the adjacent bismuth centers (**3**) is due to the bismuth attempting to satisfy its high Lewis acidity, which may be enhanced by the apparent electron withdrawing

(34) Jones, C. M.; Burkhart, M. D.; Bachman, R. E.; Serra, D. L.; Hwu, S.-J.; Whitmire, K. H. *Inorg. Chem.* **1993**, *32*, 5136–5144.

(35) Hunger, M.; Limberg, C.; Kircher, P. *Angew. Chem., Int. Ed.* **1999**, *38*, 1105–1108.

(36) Hunger, M.; Limberg, C.; Kircher, P. *Organometallics* **2000**, *19*, 1044–1050.

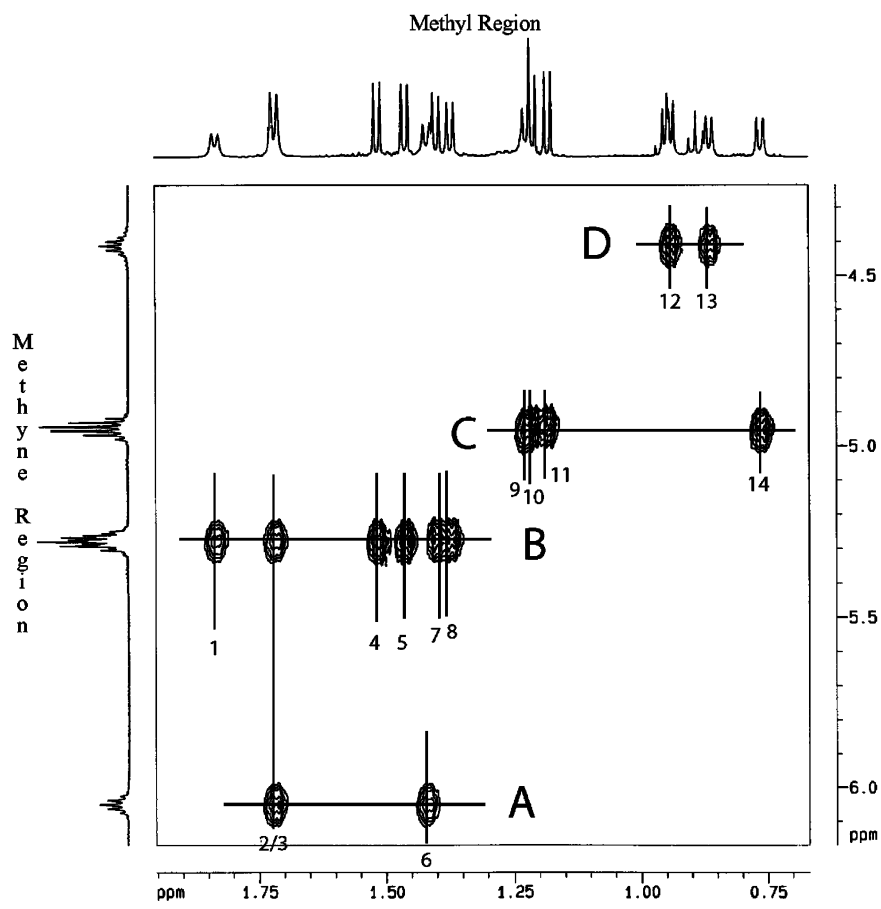


Figure 5. 2D ^1H NMR COSY of **1** in C_6D_6 showing interaction of methyne and methyl protons from the seven different isopropyl groups: The horizontal lines mark the methyne signals labeled with letters and the 14 diastereotopic methyl signals are marked with vertical lines and are represented by numbers.

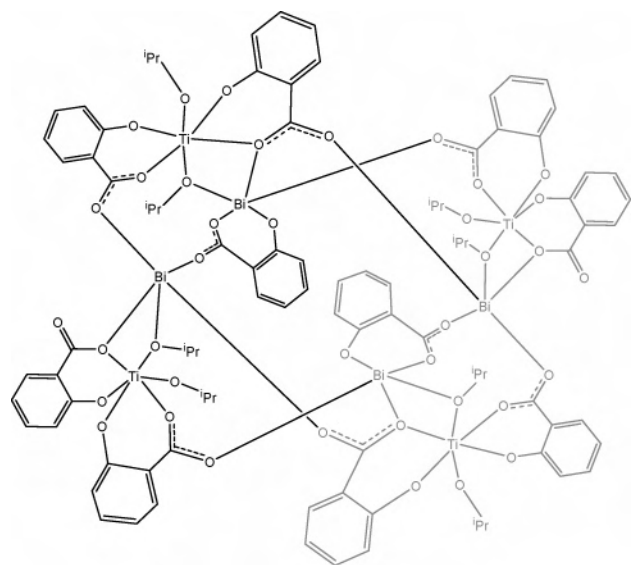


Figure 6. Line drawing highlighting the $\text{Bi}_2\text{Ti}_2(\text{sal})_2(\mu\text{-O}'\text{Pr})_2(\text{O}'\text{Pr})_2$ subunit of dimer **2**.

effects of the salicylate ligands. In other complexes that we have explored, these effects have resulted in the formation of η^6 -interactions between bismuth centers and adjacent aromatic rings.²⁷ It is not clear in this case what the factors are that have resulted in the formation of the Bi–alkoxide as opposed to the $\text{Bi}\cdots\text{aryl}$ interactions.

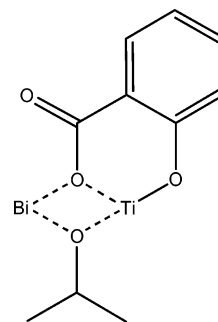


Figure 7. Line drawing of the four-centered $\text{MM}'\text{OO}'$ ring found in the solid-state structure of **2**.

The $\text{Bi}-\text{O}_{\text{alkoxide}}$ bond distance in compound **1** is 2.326(9) Å, while in complex **2**, the $\text{Bi}-\text{O}_{\text{alkoxide}}$ bond distances are 2.186(6) and 2.194(5) Å. These bond lengths compare well with the $\text{Bi}-\text{O}_{\text{alkoxide}}$ distances of 2.188(7) and 2.116(7) Å, that correspond to the bridging and terminal alkoxide ligand bond distances in $[\text{Bi}(\text{OCH}(\text{CF}_3)_2)_3\cdot\text{THF}]_2$,³⁴ and from the polymeric complex $[\text{Bi}_2(\text{acac})_2(\text{O}'\text{Pr})_4]_n$ ($d_{\text{Bi}-\text{Oalkoxide}} = 2.12(3)$ and 2.19(2) Å).²⁵ Both of these bond distances are significantly shorter than what has been observed for dative interactions between bismuth and alkoxide ligands (e.g., $d_{\text{Bi}-\text{O}} = 2.688$ Å in $[\text{Bi}(\text{OCH}(\text{CF}_3)_2)_3\cdot\text{THF}]_2$),³⁴ suggesting that the bismuth–alkoxide interaction is significantly covalent in nature. The limit of covalency in the $\text{Bi}-\text{O}_{\text{alkoxide}}$ interaction

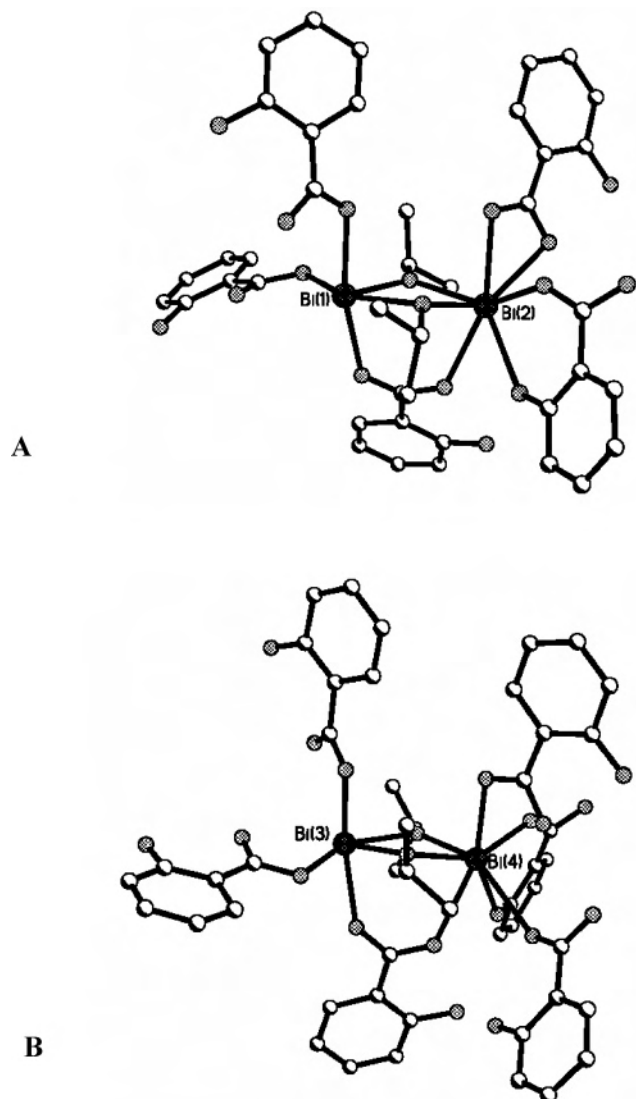


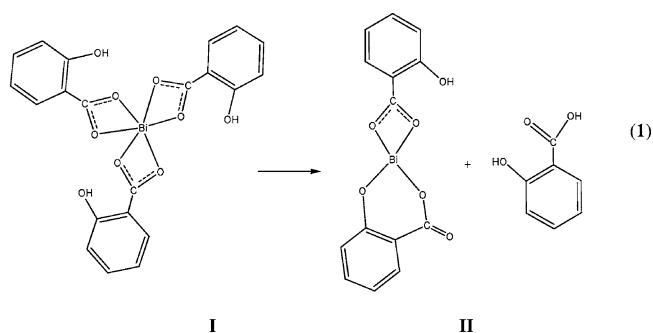
Figure 8. Binuclear bismuth subunits in **3**. Bismuth 1 and 2 (A), and bismuth 3 and 4 (B).

in these heterobimetallic complexes is observed in the solid-state structure of **3** ($d_{\text{Bi-O}} = 2.105(6)–2.136(6)$ Å).

Since complexes **2** and **3** are isomers of one another, we have considered the possibilities of how they are constructed in light of the very slow rate at which **3** is formed. We speculate that the exchange of the salicylate/alkoxide ligands between Ti and Bi may be an important step. In **2**, the Ti atoms all have the same coordination environment, $[\text{Ti}(\eta^2\text{-sal})_2(\text{OR})_2]^{2-}$, whereas in **3**, the Ti centers can all be viewed as $[\text{Ti}(\eta^2\text{-sal})_2(\eta^1\text{-sal})(\text{OR})]^{3-}$. There should be little difficulty in producing the octahedral $[\text{Ti}(\eta^2\text{-sal})_2(\text{OR})_2]^{2-}$ unit from the four-coordinate $\text{Ti}(\text{OR})_4$ starting reagent upon reaction with two salicylic acid molecules; however, to produce **3**, one more of the alkoxide ligands needs to be displaced. This substitution at the six-coordinate octahedral center may be slow.

A final facet of this investigation that merits special comment is the targeted synthesis of compound **1**, and the difficulty that we have encountered in attempting to directly synthesize complex **2** (and by extension, compound **3**) by

the same methods. Neither the solid-state nor the solution-state structure of bismuth salicylate is known with certainty. Information that we have about this compound is based upon elemental analyses of the complex itself, as well as spectroscopic and single crystal X-ray diffraction studies of the Lewis base adducts $[\text{Bi}(\text{Hsal})_3(2,2'\text{-bipyridine})\cdot\text{C}_7\text{H}_8]_2$ and $[\text{Bi}(\text{sal})(\text{Hsal})(1,10\text{-phenanthroline})\cdot\text{C}_7\text{H}_8]_2$.³⁷ What is clear from our investigations into bismuth salicylate is that the composition and reactivity of bismuth salicylate produced from the reaction of salicylic acid with triphenylbismuth varies relative to the amount of salicylic acid included in the reaction mixture; with less salicylic acid, the bismuth salicylate becomes less soluble. This is most dramatic as the ratio of bismuth to salicylic acid approaches 1:3. While NMR studies on bismuth salicylate produced from a 1:3 ratio of triphenylbismuth and salicylic acid have suggested that there is a single salicylate environment in the complex, the peaks are broad and difficult to interpret due to apparent rapid ligand exchange.²⁷ The isolation of the complexes $[\text{Bi}(\text{Hsal})_3(2,2'\text{-bipyridine})\cdot\text{C}_7\text{H}_8]_2$ and $[\text{Bi}(\text{sal})(\text{Hsal})(1,10\text{-phenanthroline})\cdot\text{C}_7\text{H}_8]_2$ from the same bismuth starting material (1:3 bismuth/salicylic acid) is more instructive, as it indicates that it is possible for bismuth salicylate to potentially exist as either the tris- or bis-salicylate complexes in association with free salicylic acid (eq 1).³⁸ At higher concentrations of



salicylic acid, such as what is required for the direct formation of complex **1**, the potential equilibrium between the two forms would be shifted in favor of form **I**, and as predicted, the heterobimetallic complex is readily produced in excellent yields. In contrast, when we targeted a ratio of 1:2.5 of triphenylbismuth to salicylic acid which is the appropriate stoichiometry required for the synthesis of complexes **2** or **3**, we always obtained insoluble products that could not be easily characterized. This suggests that, under these conditions, both **I** and **II** are present in the reaction solution leading to less regular oligomers and/or polymeric species. While other reaction mechanisms, including the ability of the free salicylic acid to interact with the bismuth center and interrupt the coordination polymer, thus enhancing the reactivity, are possible, the empirical observations fit well with such equilibrium. Indeed, it seems plausible that the coordination of the free acid with the

(37) Thurston, J. H.; Marlier, E. E.; Whitmire, K. H. *J. Chem. Soc., Chem. Commun.* **2002**, 2834–2835.

(38) Andrews, P. C.; Deacon, G. B. *J. Chem. Soc., Dalton Trans.* **2002**, 4634–4638.

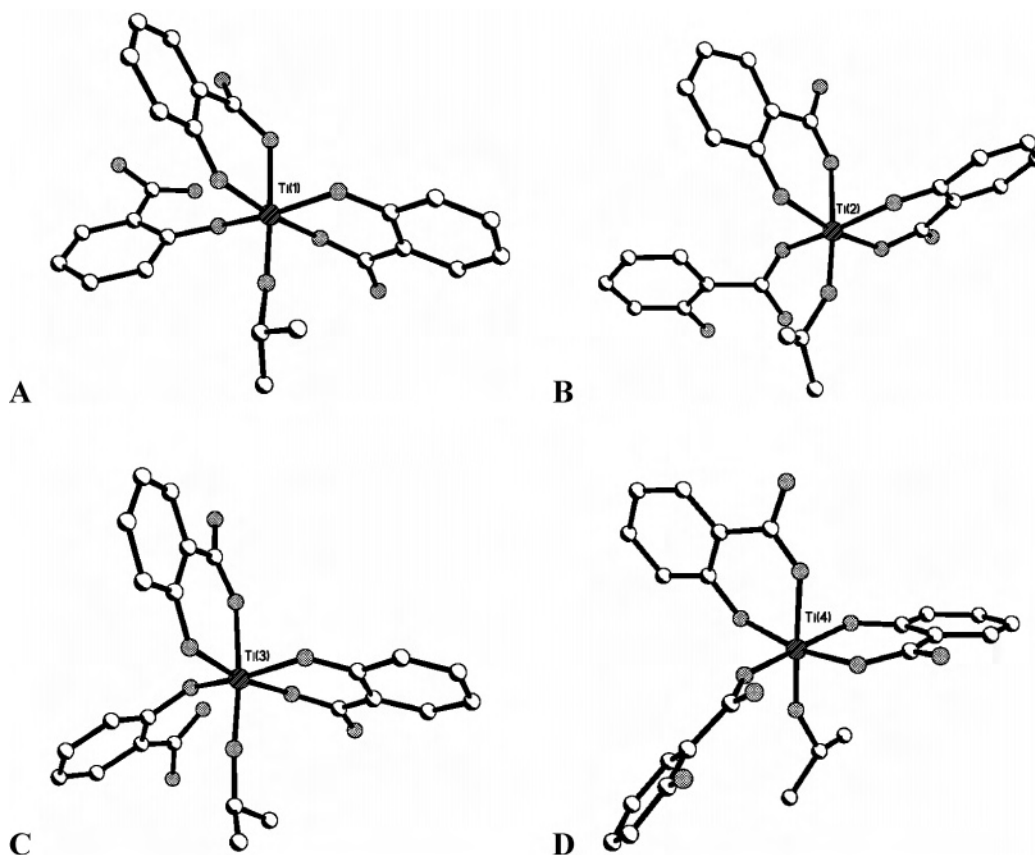


Figure 9. Titanium coordination environments in **3**. Titanium 1 (A), 2 (B), 3 (C), and 4 (D).

bismuth center and the shift in equilibrium between the two potential forms of the complex may work in tandem with one another to help direct the heterobimetallic complexes that are formed in these studies.

Conclusions

The bifunctional ligand salicylic acid is a versatile scaffold for the construction of heterobimetallic coordination complexes incorporating bismuth and titanium. In the case of **1**, the scaffold is sufficiently stable that the complex retains its solid-state structure in solution. The resulting bismuth–salicylate interaction in such complexes is labile, particularly at low concentrations of salicylic acid relative to bismuth, facilitating the exchange of ligands between the main group

and the transition metal centers, resulting in different structural motifs, and structures with different number of metal centers.

Acknowledgment. We would like to thank the Robert A. Welch Foundation and the National Science Foundation (CHE9983352) for support of this work. Dr. Larry Alemany is gratefully acknowledged for help with the NMR investigations.

Supporting Information Available: Additional NMR spectra of **1** and complete crystallographic data for compounds **1–3** in CIF format. This material is available free of charge via the Internet at <http://pubs.acs.org>.

IC049061E